

Article

Development of a Cyclic Creep Testing Station Tailored to Pressure-Sensitive Adhesives

Beatriz D. Simões ^{1,*}, Élio M. D. Fernandes ¹, Eduardo A. S. Marques ², Ricardo J. C. Carbas ^{1,*}, Steven Maul ³, Patrick Stihler ³, Philipp Weißgraeber ⁴ and Lucas F. M. da Silva ²

¹ Institute of Science and Innovation in Mechanical and Industrial Engineering (INEGI), Rua Dr. Roberto Frias, 4200-465 Porto, Portugal

² Departamento de Engenharia Mecânica, Faculdade de Engenharia, Universidade do Porto, Rua Dr. Roberto Frias, 4200-465 Porto, Portugal; lucas@fe.up.pt (L.F.M.d.S.)

³ Robert Bosch GmbH, Corporate Research and Advance Engineering, 71272 Renningen, Germany

⁴ Faculty of Mechanical Engineering and Marine Technology, University of Rostock, 18059 Rostock, Germany

* Correspondence: bsimoes@inegi.up.pt (B.D.S.); rcarbas@fe.up.pt (R.J.C.C.)

Abstract: Understanding the creep behaviour of materials is crucial in structural design, since assessing their durability and long-term performance is essential for ensuring the safety of the structures. Experimental testing allows to gather data on the creep behaviour of materials, as well as observe the damage mechanisms and dependence on environmental effects, such as stress and temperature. In this paper, the development of a cyclic creep testing station is presented. An innovative compact device is designed for testing single-lap joints using pressure-sensitive adhesives (PSAs) at different stress and temperature levels. The design is based on a mechanism that periodically supports a hanging weight resulting in an alternating load applied to the bonded joint. The assembled testing setup is validated by comparing the results of the developed machine with cyclic creep experimental data obtained with a servo-hydraulic testing machine adapted for cyclic creep. After validation, preliminary tests with one PSA at 55 °C are presented to evaluate its performance at higher temperatures. The results indicate that the developed cyclic creep machine can be used to characterise the creep behaviour of PSAs under cyclic loading.

Keywords: cyclic creep testing; pressure-sensitive adhesives; material characterisation



Citation: Simões, B.D.; Fernandes, É.M.D.; Marques, E.A.S.; Carbas, R.J.C.; Maul, S.; Stihler, P.; Weißgraeber, P.; da Silva, L.F.M.

Development of a Cyclic Creep Testing Station Tailored to Pressure-Sensitive Adhesives. *Machines* **2024**, *12*, 76. <https://doi.org/10.3390/machines12010076>

Academic Editor: Valter Carvelli

Received: 27 December 2023

Revised: 14 January 2024

Accepted: 17 January 2024

Published: 19 January 2024



Copyright: © 2024 by the authors. Licensee MDPI, Basel, Switzerland. This article is an open access article distributed under the terms and conditions of the Creative Commons Attribution (CC BY) license (<https://creativecommons.org/licenses/by/4.0/>).

1. Introduction

Comprehending the creep behaviour of materials is crucial for evaluating the long-term performance of components and structures, particularly under high-stress or high-temperature circumstances. Since metals and ceramics can creep significantly at high temperatures and polymers tend to experience creep even at low temperatures, the material that is being loaded is very significant when characterising its creep behaviour [1]. The creep phenomenon in polymers is a combination of viscous flow and elastic deformation, known as viscoelastic deformation [2], and tends to develop even at room temperature [3]. Particularly, when adhesives are subjected to long-term loading creep can occur, even for low temperatures and low stress levels [4], which leads to the material creep behaviour dependence on the service conditions [5]. Thus, any application where polymeric materials must support loads for extended periods of time while maintaining their dimensional stability has always to take creep measurements and predictions under consideration [6].

A creep curve obtained from experimental tests typically assumes three phases, named primary or transient creep, secondary or steady-state creep, and tertiary or unstable creep. These three phases appear due to the balance between strain hardening and strain softening phenomena in the material: initially the strain rate decreases due to hardening phenomena until an equilibrium between softening and hardening processes is reached, constituting the secondary creep phase. After continuum deformation in the steady-state regime, due to

the accumulated damage and necking (reduction in effective cross section due to elongation for tensile tests), the strain rate increases rapidly since the material is no longer able to withstand the applied load and eventually fails [7]. Figure 1 represents a typical creep curve where the three phases can be observed.

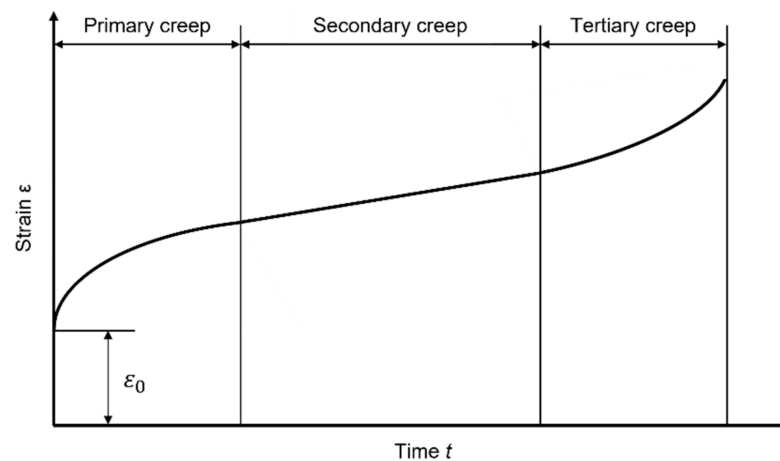


Figure 1. Schematic representation of a typical creep curve.

The shape of the curve, and thus the creep behaviour, is heavily dependent on the applied stress and testing temperature. Typically, with increasing stress, the creep time to failure decreases, and the observed strain rate increases. When increasing temperature, the creep time to failure also decreases, and the creep strain rate increases due to the increased freedom for molecular mobility and diffusion processes, depending on the material [8]. This behaviour is depicted in Figure 2, where the different colours correspond to the creep curves for the different load and temperature conditions.

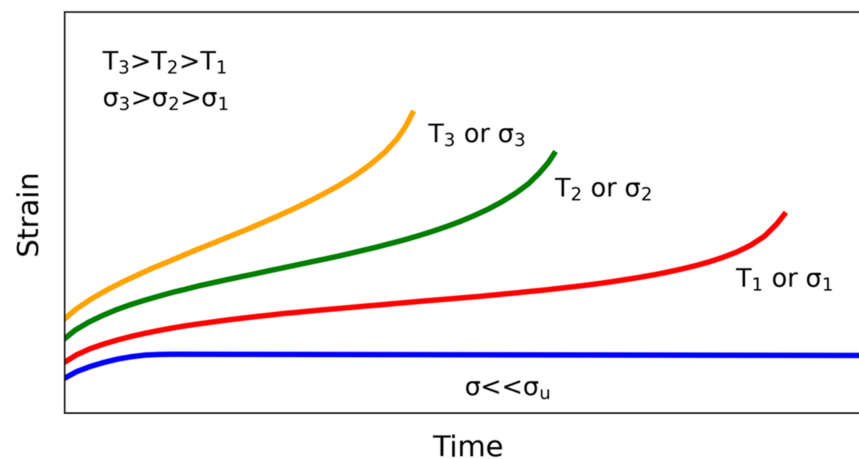


Figure 2. Influence of stress and temperature on creep behaviour.

Predicting and designing for the implications of long-term loading on deformation and failure behaviour is crucial so that, in the design phase, this phenomenon is considered for ensuring capable and safe structure for the entire service life. The experimental data needed for this safe design can be obtained from creep tests which are performed in creep testing machines or stations. This data is essential for further development of analytical and numerical models suitable for describing such behaviour [9].

Although there is some research into the static creep behaviour of PSAs, the authors are not aware, to date, of any studies into the creep mechanisms developed during cyclic loading of PSAs. This is an important phenomenon since these materials are very susceptible to creep even under service conditions of stress and temperature and cyclic loading can

have an impact on the life of the joint. If the wide range of applications of these materials is considered, from electronics to the automotive industry, the scenario of cyclic loading of structures is evident. Therefore, considering the relevance of the topic, the authors aimed to develop a machine that would allow the cyclic creep behaviour of PSAs to be characterised.

In this paper, a cyclic creep testing machine is developed for testing single-lap joints (SLJs) using pressure-sensitive adhesives (PSAs), where hanging weights are used to apply the load in the test specimen and an additional apparatus is used to control the loading and unloading of the specimen, resulting in cyclic loading. The apparatus is composed of an actuator moving a platform that supports the weight for unloading the specimen and hangs the weight to load the specimen resulting in a maximum load equal to the total weight, and a minimum of zero due to complete unloading. Then, cyclic creep tests are performed in the designed cyclic creep testing station, and the results are compared with cyclic creep tests carried out in a servo-hydraulic testing machine, to validate the developed testing machine. Finally, some preliminary results are presented for specimens tested at higher temperature with the developed cyclic machine.

2. Design of Creep Testing Machine

A creep testing machine is a structure used to perform creep tests, through the application of a constant load or stress on a specimen, with the resultant creep strain being measured over time. Creep testing setups are composed of some basic components, them being [10]:

- Grips or other fixation methods to hold the specimen in place, while assuring its alignment to properly load the specimen and accurately collect the creep deformation;
- A method to apply the load or stress that can be achieved with a hanging weight or actuators;
- A form of measuring the deformation which can be achieved with potentiometers, strain gauges, linear variable differential transformer (LVDTs), capturing photos for processing with digital image correlation (DIC), etc.;
- For testing at different temperatures, a temperature-controlled chamber can be implemented as well.

For studying the effect of other variables such as humidity or exposure to ultraviolet (UV) radiation, additional components can be implemented as well. Due to the influence of the applied stress and temperature, as well as other environmental effects, a creep testing machine can be designed to be able to adjust these variables to study its influence, with the most common variables studied being the applied stress and temperature [11–14].

Multiple designs have been proposed in the literature and industry, usually being variations of already existing designs. For instance, the creep tests can be performed under tensile [15], compressive [7], or shear loading [16]; the testing setups generally locate the specimen in a vertical position but can also employ a horizontal position [17]; the application of the load on the specimen can be carried out by hanging weights on the test specimen [18], where pulleys can also be used to relocate the weights' location. Additionally, electric or hydraulic actuators for higher loads and variable applied load [19] can be used, as well as levers to provide a mechanical advantage to apply higher loads with smaller weights [20].

For testing cyclic creep, an additional system is implemented to vary the applied load taking into account the intended characteristics of the waveform such as frequency, amplitude, waveform's shape or mean load. It is the authors' understanding that to date there is no device specially developed to test cyclic creep behaviour in PSAs. Although the study of creep behaviour in adhesives exists extensively in the literature [21–24], a detailed study of this behaviour in PSAs has not yet been carried out, even in the case of cyclic creep.

3. Design Criteria

The testing machine designed in the present work was developed to test SLJ configurations and tailored to a specific group of adhesives—PSAs. These adhesives are described

as non-structural adhesives and, therefore, when compared to structural adhesives, the strength of the materials is low. Particularly, for the PSAs expected to be used in this machine, this value is within the range of 0.2–0.7 MPa. Hence, it is expected that the required loads for the creep testing conditions are not high—never exceeding 4 kg. This means that the structural strength of the testing machine is not a major concern and can be easily achieved. Quasi-static tests performed on SLJs identical to the ones produced for cyclic creep testing provided a maximum load of around 80 N considering the two PSAs used. Another feature to consider is the maximum displacement, since these materials are highly deformable, as it was observed for some of the tested PSAs, which achieve a maximum displacement of approximately 13 mm.

The main constraint to the design was the overall dimensions of the testing station since it was meant to be placed in a temperature-controlled chamber of reduced dimensions (240 × 230 × 560 mm). For a large-scale testing setup, the testing creep station was designed to be compact and to fit three stations inside of the thermal chamber, thus simplicity and compactness were mandatory: simplicity to reduce time and costs of assembly and production of the stations, and compactness for fitting three stations in the chamber.

As for the gripping of the specimen, the grips must withstand a temperature range of testing, between −40 °C and 120 °C, and ensure good specimen alignment, with the latter being very important to reduce twisting moments on the joint which can lead to early failure.

For collecting the data from the test, the main requirements were the resolution, the ability to sustain the testing temperatures, costs, and compactness as for the overall testing station. A reasonable resolution enough to capture the strain values expected for the adhesives selected had to be defined, considering that the lowest failure strain of the preliminary tests was around 0.3. The data collecting setup must be able to withstand the same range of temperatures mentioned for the gripping system.

To specifications for the system for the cyclic loading of the adhesive joint imply that it withstands the testing temperatures as mentioned for other components of the testing station, as well as being able to support the maximum weights that are intended to be hung, corresponding to the maximum applied load for the strongest adhesive to be tested. Additionally, adjustments on the parameters of the loading cycle can be interesting to test at different frequencies and different loading and unloading stages.

4. Design Choices and Process

The final design of the creep testing setup is presented in Figure 3. This station is composed of a vertical tower with a lever component to allow for the multiplication of the applied load on the specimen, thus requiring less weights to be hung and reducing the power required for the cyclic apparatus. The vertical tower is based on a standard Bosch Rexroth 50 × 50 [mm²] aluminium profile, and was chosen since it is lightweight, strong, and an off-the-shelf product.

The grips are designed to allow for rotation in reference to the grip support, enabling for self-alignment of the grips and the joint, due to the rotation of the lever bar (Figure 3b). The grips are composed of a centred pin for aligning the joint, and two screws to then clamp the specimen between two small plates and prevent rotation and movement in relation to the grips. Additionally, the lower support for the grips is adjustable for different joint lengths as shown in Figure 3c.

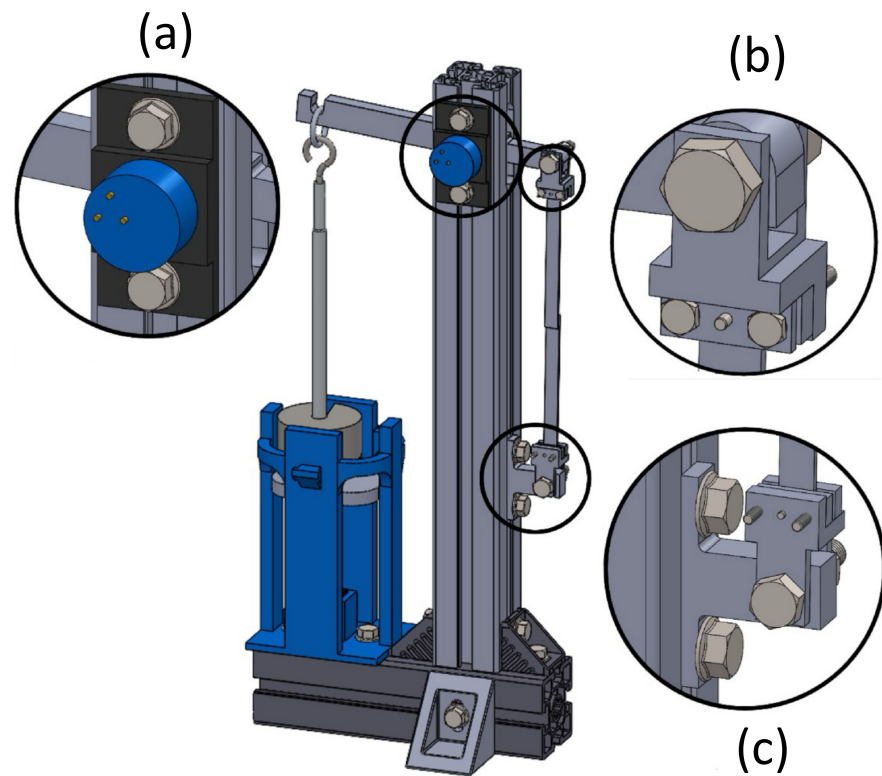


Figure 3. Cyclic creep testing machine with details: (a) potentiometer, (b) gripping system on the lever and (c) gripping system on the fixed part of the joint.

For a better understanding of the proposed configuration, Figure 4 shows the main parts of the system and their dimensions. These details make it possible to understand the different structures that make up the machine developed, as well as its overall size.

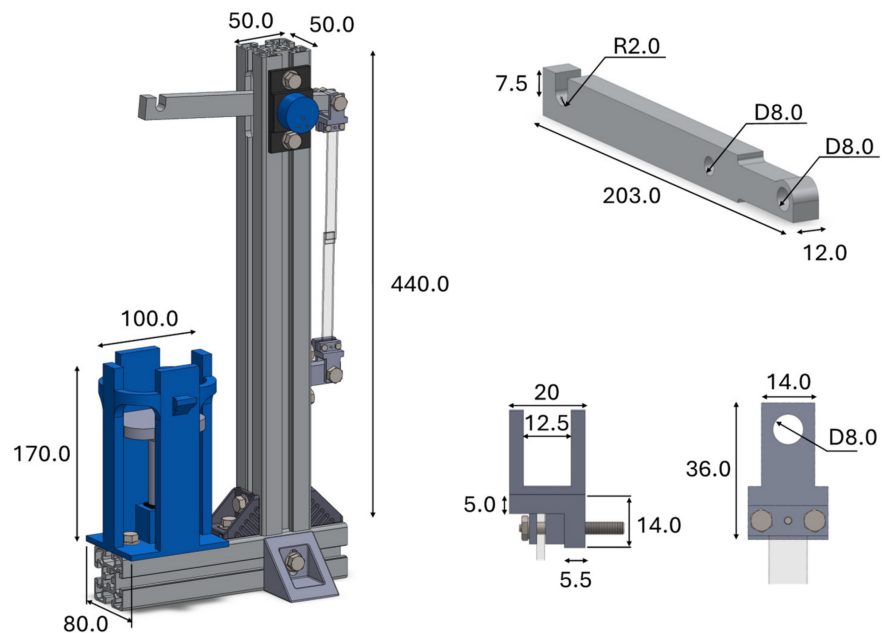


Figure 4. Different machine parts details and dimensions, in mm.

The setup for data collection is composed of an axial potentiometer (Figure 3a) that measures the angle of the lever, which can be translated to the vertical displacement at the joint by Equation (1), where K is a coefficient characteristic of the potentiometer. For

angles smaller than 13.99° or 0.2441 rad, the small angle approximation $\sin \theta \approx \theta$ induces an error of less than 1%. Considering the dimensions of the lever, this angle results in $d = 14$ mm, which is higher than the maximum displacement observed for the adhesives tested of $d = 13$ mm. Therefore, the approximation was considered valid for the presented design. Figure 5 depicts the variables used to convert the angle to vertical displacement.

$$d = b * \sin(\theta) \approx b * \theta = b * K * \Delta V_{\text{potentiometer}} \quad (1)$$

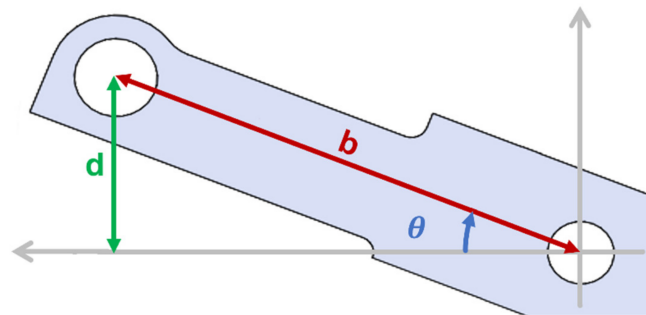


Figure 5. Diagram of conversion of angle to vertical displacement from the potentiometer voltage.

The additional system to support the hanging weight for loading and unloading the joint is composed of an electrical linear actuator, which moves the platform that supports the weight. When this platform is on the top position, the joint is unloaded and the weight is supported, and when it moves down, until the bottom position, it releases the weight and loads the joint. A guidance structure is present for aligning the platform for a vertical movement, as well as to reduce oscillation of the hanging weight when it is no longer supported, something which was observed during preliminary testing. Figure 6 shows this cyclic mechanism.

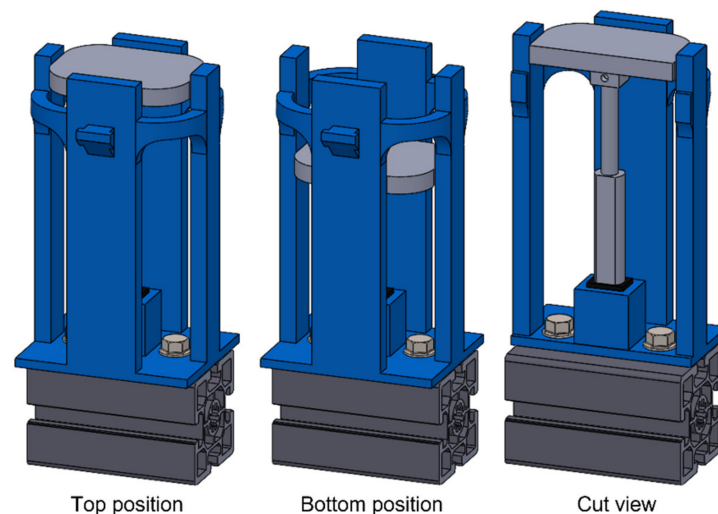


Figure 6. Design of cyclic mechanism with top and bottom positions and cut view.

For controlling the movement of the linear actuator, an additional waveform generator was used, creating a square waveform which alternates the movement of the platform in the vertical direction. The final assembly of the cyclic creep machine is shown in Figure 7.



Figure 7. Final assembly.

5. Experimental Details

To validate the cyclic creep machine designed, experimental tests of cyclic creep were conducted in both an INSTRON[®] 8801 3367 (Illinois Tool Works, Hopkinton, MA, USA) servo-hydraulic machine and the cyclic creep machine presented, for two different testing conditions. The results for each testing condition were compared for both testing setups to validate the new testing machine and verify consistency in the experimental results. After validating the new design, a set of preliminary tests were carried out in a temperature-controlled chamber, allowing to evaluate the performance of the machine at high temperature tests.

5.1. Materials and Testing Conditions

The materials used for the substrates were PMMA, also known as acrylic and aluminium. PMMA was used due to its transparency, allowing to detect defects, bubbles and voids trapped in the adhesive layer. This material is also supplied with a very flat surface, which enhances the adhesion. Its mechanical properties assume values of around 1.2 g/cm^3 for the density, 3 GPa for the Young's modulus, and 0.35 for the Poisson's ratio. The metallic substrates were produced from an aluminium alloy of the 6082-T6 series, with 2.7 g/cm^3 for the density, 70 GPa for the Young's modulus and a Poisson's ratio of 0.33 [25].

Regarding the adhesives, two different acrylic PSAs were studied: Adhesive A is a rigid acrylic transfer tape, while Adhesive B is an acrylic foam. Some characteristics of the two PSAs are presented in Table 1. The values presented were provided by the manufacturer, except for the failure load that was obtained from quasi-static SLJ tests at 1 mm/min. These results were used to calculate the values for the different load levels to be applied in the creep tests as a percentage of the strength of the adhesive.

Table 1. Characteristics of Adhesives 1 and 2.

Adhesive	Young's Modulus [MPa]	Poisson's Ratio	Density [g/cm ³]	Thickness [mm]	Maximum Quasi-Static Load [N]	Substrate
A	0.45	0.499	1.012	0.26	78.22 ± 6.75	PMMA
B	-	0.499	0.710	1.1	40.35 ± 1.17	PMMA
B	-	0.499	0.710	1.1	45.78 ± 1.71	Aluminium

The testing conditions selected for the validation of the new cyclic creep machine are defined as follows. The study of different frequencies was not included in this study.

- **Condition 1:** Adhesive A tested at 30% load level, at room temperature of 23 °C (RT).
- **Condition 2:** Adhesive B tested at 60% load level, at room temperature of 23 °C (RT).

Furthermore, Adhesive B was used to test the cyclic machine for the preliminary tests at a higher temperature. For this condition, aluminium substrates were used as PMMA cannot be tested at 55 °C as it would also undergo creep at this temperature.

- **Condition 3:** Adhesive B tested at 30% load level, at 55 °C.

5.2. Joint Assembly

Regarding the geometry of the single lap joint, Figure 8 shows the geometry and dimensions of the joints. In the image, the variable h represents the adhesive thickness of the PSA that was used for each test.

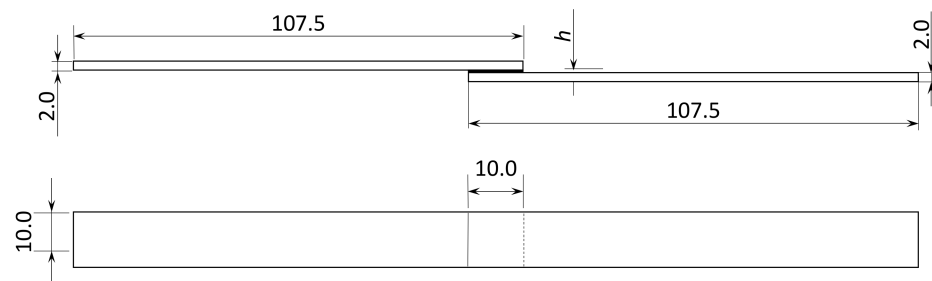


Figure 8. Geometry and dimensions of single lap joint [mm].

The surface of the acrylic substrates was initially cleaned with isopropyl alcohol to degrease and remove contaminants from the surface. Then, a $10 \times 10 \text{ mm}^2$ square of adhesive film was cut from the bulk film and the adhesive layer was pressed against one of the substrates with finger pressure. At last, to assure a good alignment and proper overlap of the single lap joints, a mould designed for this purpose was used. The assembled joints rested for 72 h with a constant pressure of 200 kPa on the overlap area over the resting period. This last step is meant to induce viscous flow of the adhesive to promote adhesion, increasing the mechanical properties of the PSAs.

5.3. Cyclic Testing Setup in Servo-Hydraulic Machine

The cyclic creep tests used as reference were carried out in an INSTRON[®] 8801 servo-hydraulic machine functioning in displacement control. To control the loading and unloading of the SLJ, the built-in trapezoidal waveform was selected to control the movement of a supporting plate that supports the weight to unload the joints, and then the platform lowers to allow the weight to hang on the joint. A schematic representation of the apparatus is presented in Figure 9 (left) and the trapezoidal waveform is depicted in Figure 9 (right).

To attach the joint to the machine, one end of the specimen was clamped to the machine's grips, while the other end was connected to the weight via a steel chain. The chain withstood the load of the weight in tension with practically no elastic strain of the component and prevented compression of the joint when the platform moved upwards and supported the weight.

There are various techniques for obtaining the adhesive displacement from experimental tests. In a previous study carried out by the authors [26], LVDT measurements were used to obtain displacement values from static creep tests. However, for cyclic creep, the DIC technique was used, since the system configuration, which is the same as the reference system for this work, was not suitable for using LVDT, and good results were obtained. DIC is a widely used technique for obtaining the field displacements of test specimens and suitable for the reference system, which is why it was chosen for this study.

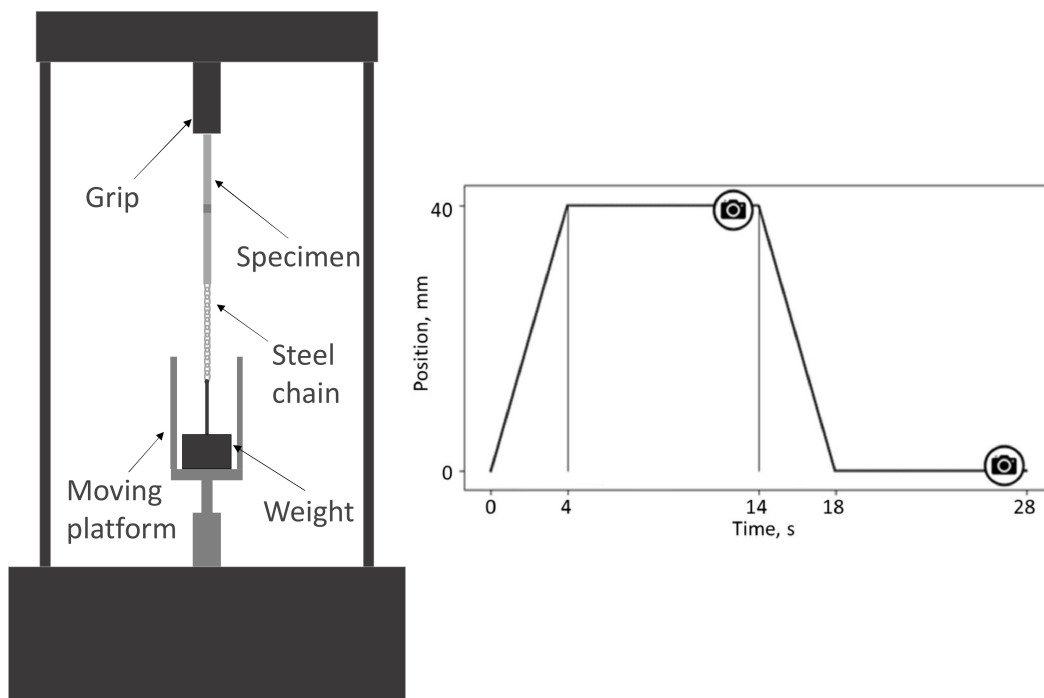


Figure 9. Schematic representation of the reference cyclic creep apparatus (left) and trapezoidal waveform implemented and moments of image capturing (right).

For these tests, one face of the joint was sprayed with matte white and a black speckle pattern, and two photographs were taken per cycle, one at the end of the loading phase and one at the end of the unloading phase, as shown in Figure 9 above. A Nikon D5300 (Tokyo, Japan) digital camera and a Nikon AF-P NIKKOR 18–55mm f/3 lens were used. The beginning and ending of the tests had to be synchronised with the beginning and ending of the images acquired in order to ensure that an accurate 2D DIC analysis could be carried out later on.

For processing the captured images and determine the displacement experienced in the joints during testing, GOM Correlate software (2019, Carl-Zeiss-Stiftung, Stuttgart, Germany) software was used. To determine the displacement in the adhesive layer, it was assumed that the deformation of both the acrylic and aluminium substrates was negligible, when compared to the deformation of the adhesive, and the substrate was considered as rigid body during testing. Thus, the measured displacement with DIC analysis, retrieved from marked points on each substrate, were equivalent to the displacement of the PSA layer.

5.4. Cyclic Testing Setup in the Developed Cyclic Creep Machine

The testing setup for the developed cyclic creep machine was composed of a power supply for the potentiometer, a waveform generator to control the linear actuator, a data acquisition system to collect and store the output voltage of the potentiometer, and the device itself. A diagram of the entire testing setup is presented in Figure 10.

The waveform generator was set to generate a square waveform with a frequency of 0.04 Hz, corresponding to a period of 28 s as it was defined in the servo-hydraulic machine; an amplitude of 6 V according to the maximum voltage defined in the specifications of the linear actuator, and a mean voltage of 0 V. The data acquisition system used was an iNet-400 InstruNet 4 Slot Card Cage (i400) (Dwyer Instruments, Michigan City, IN, USA).

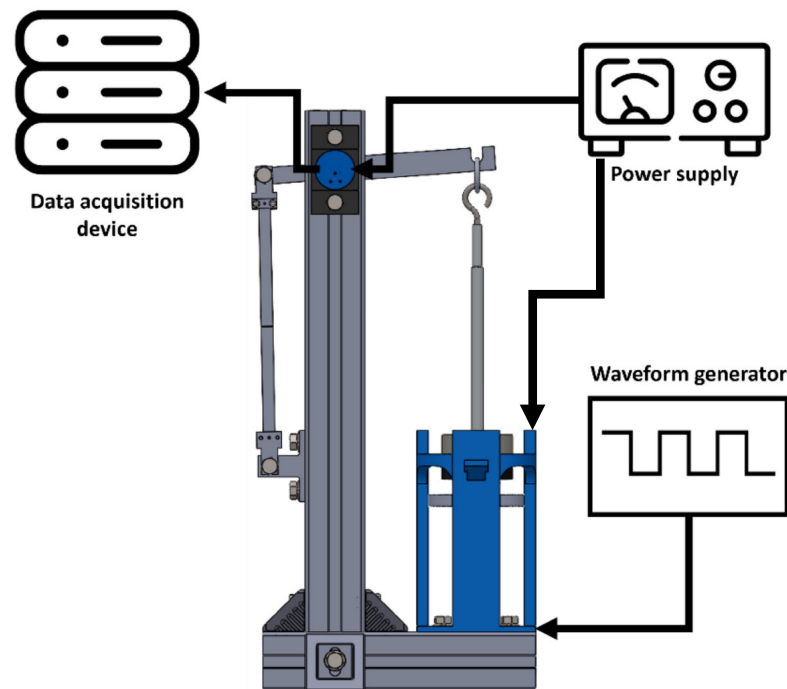


Figure 10. Diagram of cyclic creep machine setup.

5.5. Cyclic Creep Analytical Model

The displacements retrieved from both methods—DIC analysis and potentiometer—were then processed to convert the data from displacement to strain allowing to characterise the creep behaviour of the adhesives in a cyclic creep test. This conversion was performed resorting to an analytical model that the authors developed in a previous work [26]. This model allows for the characterisation of the cyclic creep behaviour of the PSAs by considering the maximum strain value for each cycle and retrieving a creep curve for the tested cyclic condition. The use of this tool allowed for a better comparison between both machines and a discussion about the validity of the developed cyclic machine for the characterisation of the cyclic creep behaviour of the adhesives and the conditions under study.

6. Experimental Results and Discussion

The experimental results for the three conditions mentioned are presented next, comparing the cyclic creep curves obtained in the servo-hydraulic machine and the cyclic creep machine under validation, as well as some preliminary results for the testing at higher temperature. It is worth noting that high values of dispersion were observed in the results, which has also been reported in the literature [5,27,28], for other research involving the study of creep behaviour of PSAs. Therefore, the shape of the curve and, thus, the characteristic creep behaviour of the adhesive is more relevant to validate the cyclic creep machine rather than the time to failure or strain. The behaviour observed in both machines must be similar, which should translate into similar shapes of the curves obtained, although there may be slight variations in the strain to failure and large variations in the time to failure.

6.1. Adhesive A at 30% Load Level and RT

The results from cyclic creep testing of Adhesive A at 30% load level and RT are shown in Figures 11 and 12, with the first plot presenting the tests performed in the servo-hydraulic machine (the apparatus used as reference) and the second presenting the tests in the cyclic creep machine under validation.

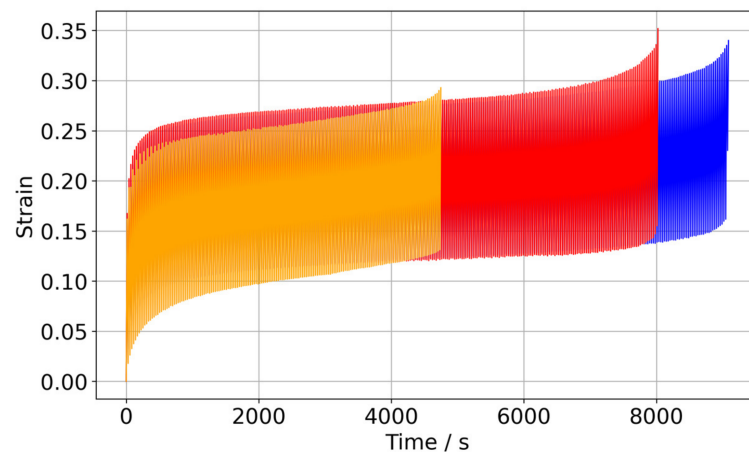


Figure 11. Cyclic creep results for Adhesive A at 30% load level and RT in servo-hydraulic machine, where each colour represents a different test.

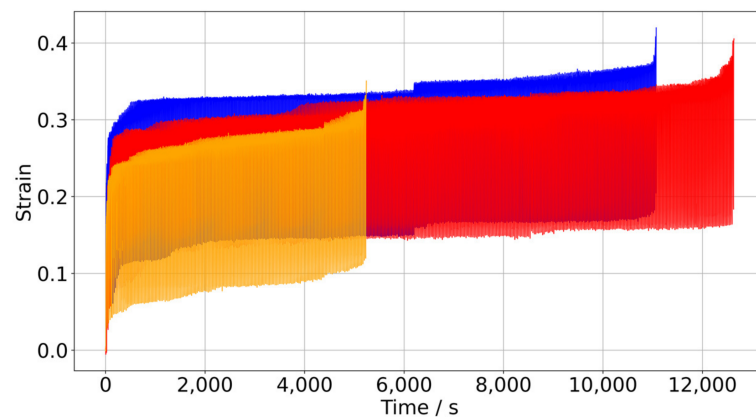


Figure 12. Cyclic creep results for Adhesive A at 30% load level and RT in cyclic creep machine, where each colour represents a different test.

From the curves presented in Figures 11 and 12, similar failure strain values can be observed, whose values vary between about 0.30 and 0.40. However, as mentioned before, this adhesive presents large experimental dispersion under creep and, therefore the time to failures vary substantially. Additionally, after a big testing campaign, it was possible to conclude that Adhesive A is very sensitive to defects and air entrapment and a good repeatability in time to failure was harder to achieve. In what concerns the shape of the curve, there was good agreement, as every curve obtained from experimental testing presented a similar trend, being possible to capture the almost constant amplitude of the deformation throughout the entire curve, except for the tertiary phase, which seems to be a characteristic of this adhesive, for the load level and frequency under testing. This is visible in every curve shown in Figures 11 and 12.

By selecting the shortest curve from each plot due (with similar failure time), a comparison of the results can be carried out more clearly, where it is visible that the top and bottom parts of the curves are almost parallel due to the near constant amplitude throughout the duration of the test (Figure 13). The almost constant amplitude of the strain values, indicate that this adhesive can recover almost all of the deformation, until the tertiary phase where failure occurs. This would be a cyclic creep property of the material and thus the test setup needs to be able to capture this characteristic behaviour.

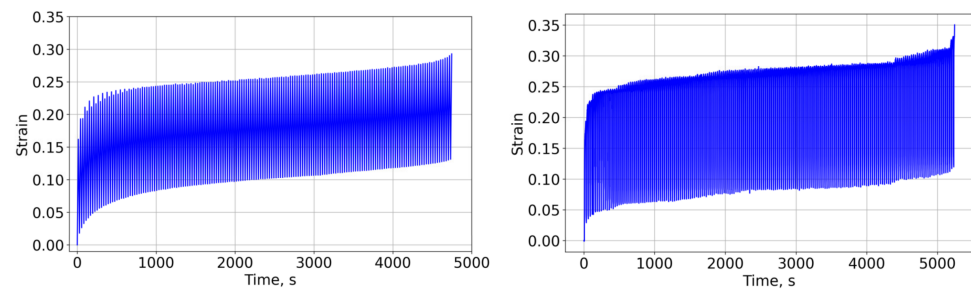


Figure 13. Cyclic creep curves for Adhesive A at 30% load level and RT: **(left)** servo-hydraulic and **(right)** cyclic creep machine.

Since this condition corresponds to 30% of the adhesive strength under quasi-static loading, it was expected that the creep curve should present a stable secondary phase. This corresponds to a very low value for the strain rate and the capacity for the material to withstand this load without damage initiation and propagation, which corresponds to the tertiary phase of the curve. It is possible to observe in Figure 14 that both testing machines performed as expected, generating curves with a very stable secondary phase.

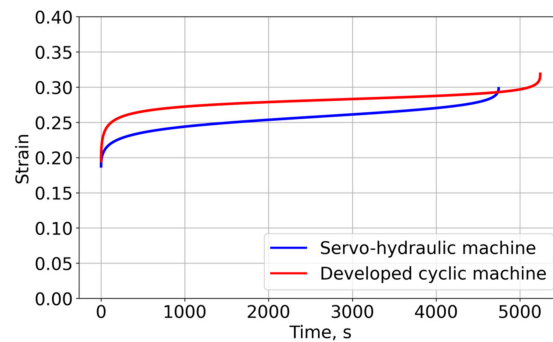


Figure 14. Cyclic creep curves retrieved from the model for testing with both machines of Adhesive A.

By analysing the results, it can be concluded that the proposed setup achieved the desired results for the tested condition, with the results presenting a good level of agreement. In this way, the setup together with the model used to generate the creep curves could be used to analyse the cyclic creep behaviour in further testing.

6.2. Adhesive B at 60% Load Level and RT

The experimental cyclic creep curves from Adhesive B at 60% load level and RT are shown in Figure 15 for the servo-hydraulic machine (three tests), and Figure 16 for the cyclic creep machine under validation (four tests).

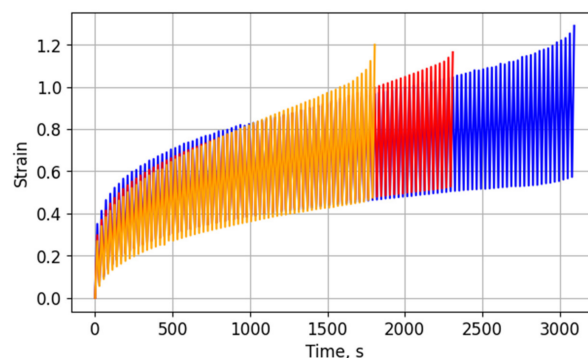


Figure 15. Cyclic creep results for Adhesive B at 60% load level and RT in servo-hydraulic machine, where each colour represents a different test.

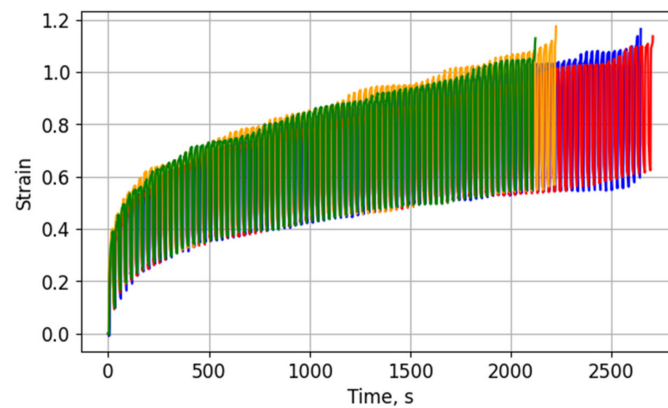


Figure 16. Cyclic creep results for Adhesive B at 60% load level and RT in cyclic creep machine, where each colour represents a different test.

In the plots above, the failure strain is more consistent in comparison to Adhesive A, assuming values of approximately 1.1 to 1.2. Also, this material presents higher values of deformation when compared to Adhesive A since it is an acrylic foam adhesive, unlike Adhesive A which is a stiffer transfer tape, and due to the increased thickness. Similar to Adhesive A, the experimental tests also returned some dispersion for the time to failures, although Adhesive B performed in a more consistent way. Regarding the shape of the curve, the amplitude increased with time since the primary stage, showing a different behaviour when compared to Adhesive A, which presented a constant amplitude through the test. As for the Adhesive A, this is a characteristic behaviour of the material, being a cyclic creep property, that can be used to characterise the adhesive. This behaviour can be detected in all of the tests depicted in Figures 15 and 16. Selecting one curve from each plot above with similar time to failures, the resemblances between the curves are easily observed (Figure 17). These results enhance the capability of the developed setup to be used to characterise the cyclic creep behaviour of PSAs under cyclic creep loading.

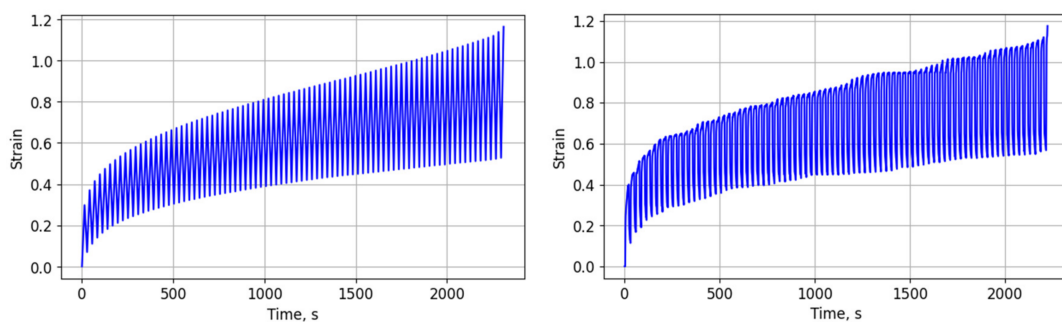


Figure 17. Cyclic creep curves for Adhesive B at 60% load level and RT: (left) servo-hydraulic and (right) cyclic creep machine.

Since Adhesive B was tested at a higher load level when compared to Adhesive A, the shape of the creep curve should present some different characteristics. When loaded with 60% of static strength of the adhesive, it was expected that the values of the strain rate during the secondary phase should be higher than those encountered for lower load levels, resulting in a less stable phase with a higher slope. Consequently, there is a bigger contribution of primary and secondary phases in these conditions, with a less developed secondary phase. Figure 18 shows the results of testing in both machines for the condition tested with Adhesive B.

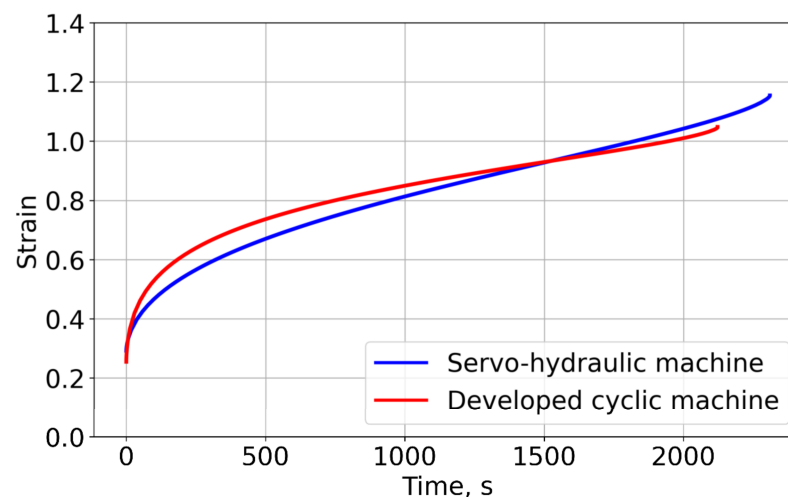


Figure 18. Cyclic creep curves retrieved from the model for testing with both machines of Adhesive B.

The obtained results using the developed machine together with the cyclic creep model indicate that the setup is able to generate valid curves for the tested condition with Adhesive B. The applied load level should result in curves with shapes as presented in Figure 18. Additionally, the resulted curves present a very good agreement, suggesting that the setup is also suitable to test higher load level conditions.

6.3. Adhesive B at 30% Load Level and 55 °C

Since the developed cyclic machine was able to perform as expected with the results being validated with a reference machine, the tests for condition 3 were only performed with the new apparatus. The preliminary tests for high temperature were also conducted with aluminium substrates, since PMMA was unable to withstand the higher temperature, and the results of two tests can be observed in Figure 19.

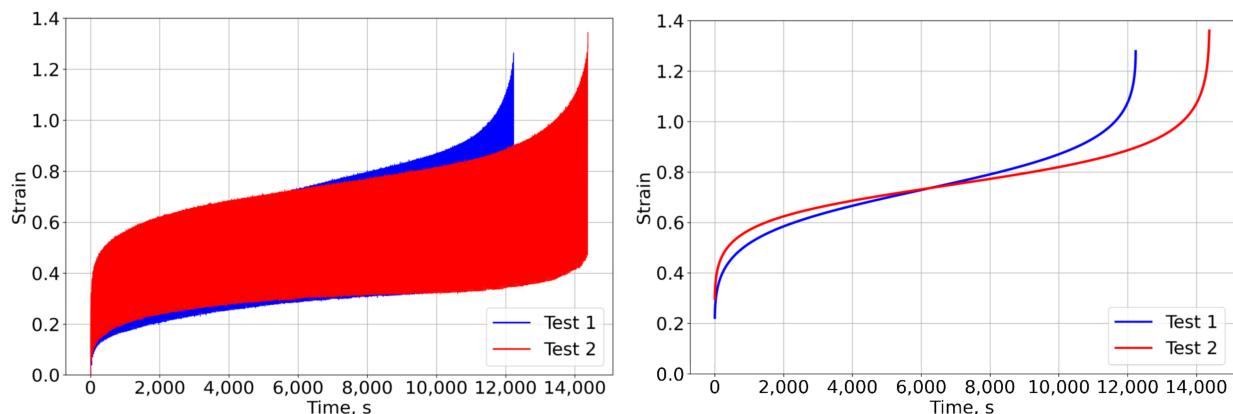


Figure 19. Cyclic creep results for Adhesive B at 30% load level and 55 °C in cyclic creep machine: cyclic test (left) and the respective creep curve (right).

From Figure 19 on the left, it is possible to observe that the two tests presented good repeatability both for strain to failure and failure time. As expected, there are some variations in the failure time since it is a frequent characteristic of creep testing in PSAs. However, this variation is acceptable from the repeatability point of view, with very consistent values for the strain to failure, varying between approximately 1.26 and 1.34. Figure 19 on the right depicts the creep curves that can be retrieved from the cyclic creep model when fed with the experimental results from the cyclic machine. In this image, it is also clear that both tests present almost coincident curves, with the failure time being the

only changing variable. Since this is not induced by the apparatus, as previously validated, the suitability of the machine for this condition can also be assumed.

6.4. Comparison between Two Conditions for Adhesive B

Figure 20 shows the comparison between one test for each condition 2 and 3. The blue line represents the condition with 60% load level at RT and the red line represents the condition with 30% load level at 55 °C. This final comparison was performed to determine if the shape and trends obtained in the creep curves were consistent with what is described in the literature.

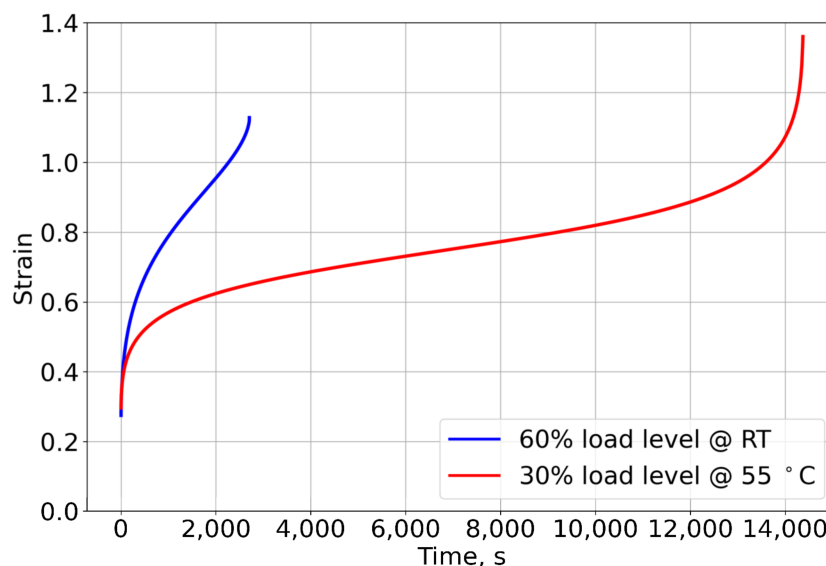


Figure 20. Comparison of the creep curves between condition 2 and condition 3.

By observing Figure 20, it becomes evident that the shape, the strain to failure, and the failure time are all affected by the change in the testing conditions. Regarding the shape of the curve, an increase in the development of the secondary phase for the 30% load level can be seen, which is in accordance with a more favourable stress state, presenting a slower progression of the strain levels. This behaviour also explains the difference in the failure time, which is 5.3 times higher for the lower load level. Finally, the increase of the strain to failure is explained by the temperature at which the test was performed. By increasing the temperature, the material becomes softer and there is a higher mobility of the polymer chains, which induces higher deformations before failure.

The creep curves obtained for the different conditions indicate that the machine is valid and, together with the model, can be used to characterise the cyclic creep behaviour of PSAs.

7. Conclusions

In this paper, a cyclic creep machine was designed to characterise the cyclic creep behaviour of SLJs bonded with PSAs. The aim was to develop a machine that would be easy to assemble, low-cost and compact, allowing for an easy assemble of multiple stations and enhancing the test capability. However, PSAs have unique characteristics, due to their viscoelastic properties that enable big deformations and even for small size specimens the machine needs to be suitable for big displacements.

In order to validate the design, creep tests were carried out for two different adhesives and load levels, and the results were compared with those obtained with a servo-hydraulic machine adapted for cyclic creep tests. Tests were carried out on both adhesives at RT: Adhesive A at 30% load level and Adhesive B at 60% load level.

- The shape of the cyclic curves seems to be characteristic of each adhesive and has been captured by the new design, with results similar to those obtained with the reference machine;
- When the characteristic creep curves of the adhesive are compared for the condition under analysis, both the experimental data from Adhesive A and Adhesive B generate very similar curves between the two apparatus.

Following validation of the new apparatus, additional preliminary tests were conducted to test the device at higher temperature. The results for 30% load level and 55 °C on Adhesive B allowed to add some conclusions:

- The tests presented similar failure times with a very small variation in the failure strain. Moreover, the creep curves generated with the experimental data presented very similar shapes and values, yielding a very good agreement;
- When comparing the two conditions conducted using Adhesive B, there was a significant increase in failure time, as well as a more developed secondary phase for the condition with a lower load level;
- Finally, an increase in strain to failure was also observed for the higher temperature condition, which is compatible with a greater molecular mobility of the polymer chains.

The results in the present study indicate that the developed cyclic creep machine can be used to characterise the cyclic creep behaviour of PSAs. The machine's structures have proved capable of withstanding the loads and temperatures applied, and both the potentiometer and the actuator have obtained accurate data that has been validated with reference results. Among the possibilities of this new design is the fact that it makes it possible to vary the level of load applied to the joint, the temperature at which it is tested, and especially the frequency with which the load cycles occur. In this paper, the study of the influence of frequency was not included, so it would be interesting as a future work for a complete characterisation of these materials when loaded in cyclic conditions.

Author Contributions: Conceptualization, É.M.D.F., E.A.S.M., R.J.C.C., S.M., P.S., P.W. and L.F.M.d.S.; Methodology, B.D.S., É.M.D.F., E.A.S.M., R.J.C.C., S.M., P.S., P.W. and L.F.M.d.S.; Software, É.M.D.F.; Validation, B.D.S., É.M.D.F., E.A.S.M., R.J.C.C., S.M., P.S., P.W. and L.F.M.d.S.; Formal analysis, B.D.S.; Investigation, B.D.S. and É.M.D.F.; Resources, S.M., P.S. and L.F.M.d.S.; Data curation, B.D.S. and É.M.D.F.; Writing—original draft, B.D.S. and É.M.D.F.; Writing—review & editing, E.A.S.M., R.J.C.C., S.M., P.S., P.W. and L.F.M.d.S.; Supervision, E.A.S.M., R.J.C.C., S.M., P.S., P.W. and L.F.M.d.S.; Project administration, S.M., P.S. and L.F.M.d.S.; Funding acquisition, S.M., P.S. and L.F.M.d.S. All authors have read and agreed to the published version of the manuscript.

Funding: The authors gratefully acknowledge the Portuguese Foundation for Science and Technology (FCT) for supporting the work presented here through the individual grant 2023.03694.BD.

Data Availability Statement: The data presented in this study are available on request from the corresponding author. The data presented in this study are available on request from the corresponding author (legal reasons).

Acknowledgments: The authors wish to acknowledge and thank the support provided by Robert Bosch GmbH, Corporate Research and Advance Engineering, Renningen.

Conflicts of Interest: Authors Steven Maul and Patrick Stihler were employed by the company Robert Bosch GmbH. The remaining authors declare that the research was conducted in the absence of any commercial or financial relationships that could be construed as a potential conflict of interest.

References

1. Paupler, P. Book Review: Dieter, G.E. *Mechanical Metallurgy*, 3rd ed.; Mc Graw-Hill Book Co., Ltd.: New York, NY, USA, 1986; p. XXIII + 751; DM 138.50; ISBN 0-07-016893-8. *Cryst. Res. Technol.* **1988**, *23*, 194. [\[CrossRef\]](#)
2. Wang, W.-H.; Huang, H.-B.; Du, H.-H.; Wang, H. Effects of fiber size on short-term creep behavior of wood fiber/HDPE composites. *Polym. Eng. Sci.* **2015**, *55*, 693–700. [\[CrossRef\]](#)
3. Vakili-Tahami, F.; Adibeig, M.R. Using developed creep constitutive model for optimum design of HDPE pipes. *Polym. Test.* **2017**, *63*, 392–397. [\[CrossRef\]](#)

4. Khoramishad, H.; Ashofteh, R.S. Influence of multi-walled carbon nanotubes on creep behavior of adhesively bonded joints subjected to elevated temperatures. *J. Adhes.* **2019**, *95*, 979–994. [[CrossRef](#)]
5. Ortega-Iguña, M.; Chludzinski, M.; Sánchez-Amaya, J.M. Comparative Mechanical Study of Pressure Sensitive Adhesives over Aluminium Substrates for Industrial Applications. *Polymers* **2022**, *14*, 4783. [[CrossRef](#)]
6. Kolařík, J.; Pegoretti, A. Proposal of the Boltzmann-like superposition principle for nonlinear tensile creep of thermoplastics. *Polym. Test.* **2008**, *27*, 596–606. [[CrossRef](#)]
7. Duan, X.; Yuan, H.; Tang, W.; He, J.; Guan, X. A Phenomenological Primary–Secondary–Tertiary Creep Model for Polymer-Bonded Composite Materials. *Polymers* **2021**, *13*, 2353. [[CrossRef](#)] [[PubMed](#)]
8. Callister, W.D., Jr. *Materials Science and Engineering an Introduction*; John Wiley: Hoboken, NJ, USA, 2007.
9. Dean, G.; Broughton, W. *A Review of Creep Modelling for Toughened Adhesives and Thermoplastics*; ResearchGate: Berlin, Germany, 2005.
10. Broughton, W.; Dean, G. *Fatigue and Creep Testing of Adhesives and Thermoplastic Joined Systems*; ResearchGate: Berlin, Germany, 2023.
11. Sadigh, M.A.S.; Paygozar, B.; da Silva, L.F.M.; Martínez-Pañeda, E. Creep behaviour and tensile response of adhesively bonded polyethylene joints: Single-Lap and Double-Strap. *Int. J. Adhes. Adhes.* **2020**, *102*, 102666. [[CrossRef](#)]
12. Emara, M.; Torres, L.; Baena, M.; Barris, C.; Moawad, M. Effect of sustained loading and environmental conditions on the creep behavior of an epoxy adhesive for concrete structures strengthened with CFRP laminates. *Compos. Part B Eng.* **2017**, *129*, 88–96. [[CrossRef](#)]
13. Wu, C.; Wu, R.; Xia, W.; Tam, L. Understanding Creep Behavior of Semicrystalline Polymer via Coarse-Grained Modeling. *J. Polym. Sci. Part B Polym. Phys.* **2019**, *57*, 1779–1791. [[CrossRef](#)]
14. Tan, W.; Na, J.-X.; Zhou, Z.-F. Effect of temperature and humidity on the creep and aging behavior of adhesive joints under static loads. *J. Adhes.* **2022**, *99*, 672–690. [[CrossRef](#)]
15. Costa, I.; Barros, J. Tensile creep of a structural epoxy adhesive: Experimental and analytical characterization. *Int. J. Adhes. Adhes.* **2015**, *59*, 115–124. [[CrossRef](#)]
16. Deshpande, A.; Song, Z.; Vaidya, S. A Creep Model for Pressure Sensitive Adhesives Under Shear Load. In Proceedings of the 2020 Asia-Pacific International Symposium on Advanced Reliability and Maintenance Modeling (APARM), Vancouver, BC, Canada, 20–23 August 2020; ResearchGate: Berlin, Germany, 2020; pp. 1–5. [[CrossRef](#)]
17. Presby, M. *Design of a Horizontal Creep Testing Machine*; The University of Akron: Akron, OH, USA, 2015.
18. Ernault, E.; Diani, J.; Schmid, Q. Single-lap joint creep behaviour of two soft adhesives. *J. Adhes.* **2022**, *99*, 1282–1289. [[CrossRef](#)]
19. Bezerra, G.N.; da Silva, C.M.M.; Lopes, A.M.; Da Silva, L.F.; Marques, E.A.; Carbas, R.J.; Nunes, P.D. Development of a Multi-Station Creep Machine for Adhesive Joint Testing. *J. Test. Eval.* **2022**, *50*, 2382–2399. [[CrossRef](#)]
20. Duncan, B.; Maxwell, A. *Measurement Methods for Time-Dependent Properties of Flexible Adhesives*; ResearchGate: Berlin, Germany, 1999.
21. Aicher, S.; Christian, Z.; Stapf, G. Creep Testing of One-Component Polyurethane and Emulsion Polymer Isocyanate Adhesives for Structural Timber Bonding*. *For. Prod. J.* **2015**, *65*, 60–71. [[CrossRef](#)]
22. Marques, E.A.S.; Carbas, R.J.C.; Silva, F.; da Silva, L.F.M.; de Paiva, D.P.S.; Magalhães, F.D. Use of master curves based on time-temperature superposition to predict creep failure of aluminium-glass adhesive joints. *Int. J. Adhes. Adhes.* **2017**, *74*, 144–154. [[CrossRef](#)]
23. Khabazaghdam, A.; Behjat, B.; Yazdani, M.; Da Silva, L.F.M.; Marques, E.A.S.; Shang, X. Creep behaviour of a graphene-reinforced epoxy adhesively bonded joint: Experimental and numerical investigation. *J. Adhes.* **2021**, *97*, 1189–1210. [[CrossRef](#)]
24. Feng, C.-W.; Keong, C.-W.; Hsueh, Y.-P.; Wang, Y.-Y.; Sue, H.-J. Modeling of long-term creep behavior of structural epoxy adhesives. *Int. J. Adhes. Adhes.* **2005**, *25*, 427–436. [[CrossRef](#)]
25. MIT Library. 6.777/2.751] *Material Properties Database*; MIT Library: Cambridge, MA, USA. Available online: <https://www.mit.edu/~6.777/matprops/matprops.htm> (accessed on 1 July 2023).
26. Simões, B.D.; Fernandes, É.M.; Marques, E.A.; Carbas, R.J.; Maul, S.; Stihler, P.; Weißgraeber, P.; da Silva, L.F. An Exploratory Study on Determining and Modeling the Creep Behavior of an Acrylic Pressure-Sensitive Adhesive. *Materials* **2023**, *16*, 2029. [[CrossRef](#)]
27. Townsend, B.W.; Ohanehi, D.C.; Dillard, D.A.; Austin, S.R.; Salmon, F.; Gagnon, D.R. Characterizing acrylic foam pressure sensitive adhesive tapes for structural glazing applications—Part I: DMA and ramp-to-fail results. *Int. J. Adhes. Adhes.* **2011**, *31*, 639–649. [[CrossRef](#)]
28. Huang, H.; Dasgupta, A.; Singh, N. Predictive Mechanistic Model of Creep Response of Single-Layered Pressure-Sensitive Adhesive (PSA) Joints. *Materials* **2021**, *14*, 3815. [[CrossRef](#)]

Disclaimer/Publisher’s Note: The statements, opinions and data contained in all publications are solely those of the individual author(s) and contributor(s) and not of MDPI and/or the editor(s). MDPI and/or the editor(s) disclaim responsibility for any injury to people or property resulting from any ideas, methods, instructions or products referred to in the content.